

MAGNETOSTRICTIVE DAMPING OF TWO FERROMAGNETIC  
ALLOYS AT ELEVATED TEMPERATURES

by

NEWTON REED ANDERSON

B.S., Kansas State University, 1958

---

A MASTER'S REPORT

submitted in partial fulfillment of the  
requirements for the degree

MASTER OF SCIENCE

Department of Mechanical Engineering

KANSAS STATE UNIVERSITY  
Manhattan, Kansas

1966

Approved by:

  
Major Advisor

LD  
2668  
R4  
1966  
A548  
C.2

TABLE OF CONTENTS

NOMENCLATURE . . . . .	iii
INTRODUCTION . . . . .	1
METHODS OF DEFINING INTERNAL DAMPING . . . . .	3
FACTORS AFFECTING INTERNAL DAMPING . . . . .	5
MAGNETOSTRICTIVE DAMPING . . . . .	7
EFFECT OF TEMPERATURE ON MAGNETOSTRICTIVE DAMPING. . . . .	10
DEFINITION OF PROBLEFM. . . . .	11
EXPERIMENTAL PROCEDURE . . . . .	14
DISCUSSION OF RESULTS . . . . .	20
CONCLUSIONS . . . . .	22
ACKNOWLEDGEMENT . . . . .	23
REFERENCES . . . . .	24
APPENDIX . . . . .	25
A. Calibration Procedure . . . . .	25
B. Equipment List . . . . .	32
C. Typical Data . . . . .	34
D. Determination of Magnetic Saturation . . . . .	36
E. Derivation of Logarithmic Decrement . . . . .	41

## NOMENCLATURE

$\delta$	logarithmic decrement, dimensionless
n	number of cycles
Ln	natural logarithm
$A_0$	initial amplitude, centimeters
$A_n$	amplitude after n cycles, centimeters
$\Psi$	specific damping capacity, dimensionless
W	total vibrational energy, inch pounds per cubic inch
$\Delta W$	energy loss per cycle, inch pounds per cubic inch
$A_r$	resonant amplification factor, dimensionless
$K_m$	material factor, equation (5), dimensionless
$K_c$	cross sectional shape factor, equation (5), dimensionless
$K_s$	longitudinal stress distribution factor, equation (5), dimensionless
$K_E$	energy absorption function, equation (6), dimensionless
$K_\sigma$	stress distribution function, equation (6), dimensionless
D	specific damping energy, inch pounds per cubic inch per cycle
J	material constant, equation (7), dimensionless
N	material constant, equation (7), dimensionless
S	stress, pounds per square inch
M	bending moment, inch pounds
P	bending load, pounds
l	length, inches
Z	section modulus, cubic inches
d	diameter of rod, inches

$\omega$  damped natural frequency, radians per second  
 $x$  amplitude of vibration, inches  
 $c$  damping coefficient, pound-seconds per inch  
 $k$  spring constant, pounds per inch  
 $t$  time, seconds  
 $m$  mass, pounds

## INTRODUCTION

Damping capacity, or internal damping, can be defined as that property of solid material which results in energy absorption when the material is subjected to a cyclic stress. Damping capacity can be of prime importance in keeping down the amplitude of vibratory motion, and therefore the stress magnitude of a vibrating member. Despite the significance of internal damping, very little has been done to describe it analytically, probably because of the large number of parameters involved and the lack of general functional relationships.

As early as 1865, Lord Kelvin [1] had formulated the conception that damping in solids was a phenomena associated with a viscous force proportional to the strain velocity. He arrived at this conclusion through analogy with viscous friction in fluids. His own experiments, however, failed to support his theory. Damping was first presented as a hysteresis phenomenon in 1912 by Hopkinson and Williams [2] by noting that the stress strain diagram for a complete cycle was a closed loop and was analogous to magnetic hysteresis.

To determine the damping capacity of a material, Föppl [3] assumed that any strain is composed of an elastic portion and a plastic portion, the plastic portion causing the energy loss. This plastic portion being non-recoverable is dissipated into heat.

In more recent literature, Gochardt [6] and Lazan [5] developed analytical expressions for internal damping based on the stress resonant amplification factor as a function of stress distribution, shape of

[ ] Numbers in brackets designate references at end of report.

member, and a material factor. These approaches, however, are dependent on the accurate measurement of stress distribution and a knowledge of the energy absorbing characteristics of the material. Obtaining meaningful results analytically for complicated shapes and loadings is extremely difficult, not only due to the difficulty in defining the stress distribution, but also due to the other variables which affect internal damping such as variability of stress history, machining stresses, variation in material properties, and stress concentrations.

## METHODS OF DEFINING INTERNAL DAMPING

A great many investigators have made measurements of the rate of vibration decay of free vibration, or logarithmic decrement which is probably the best known of the methods of determining internal damping and is the easiest quantity to determine experimentally. See Appendix E for derivation of the logarithmic decrement. If  $A_0$  and  $A_n$  are the amplitudes of vibration  $n$  cycles apart, then

$$\delta = \frac{1}{n} \ln \frac{A_0}{A_n} \quad (1)$$

Föppl [3] presented his data in terms of the specific damping capacity although his measurements were of vibration decay. Specific damping capacity is defined as the ratio of energy loss per cycle to the vibrational energy of the member.

$$\psi = \frac{\Delta W}{W} \quad (2)$$

Lazan [4] showed that the following relationship existed between the logarithmic decrement and the specific damping capacity.

$$\psi = 2 \left[ \delta + \delta^2 + \left( \frac{2\delta^3}{3} \right) + \dots \right] \quad (3)$$

If the magnitude of  $\delta$  is small as in most engineering metals, equation (3) can be reduced to

$$\psi = 2 \delta \quad (4)$$

If  $\delta$  is large in magnitude, as in most plastics, then a greater number of terms must be kept.

For a sustained vibration, the most convenient and meaningful method of defining internal damping is the resonance amplification

factor. Lazan [5] defines the resonance amplification factor to be

$$A_r = K_m K_c K_s \quad (5)$$

where  $K_m$  is a factor which depends on the material characteristics,  $K_c$  is dependent on the cross sectional shape of the specimen, and  $K_s$  is dependent on the longitudinal stress distribution. Cocharde [6], bases his analysis of the resonance amplification factor on two quantities, a stress distribution function,  $K_\sigma$ , and an energy absorption function,  $K_E$ . His definition then becomes

$$A_r = K_E K_\sigma \quad (6)$$

Other methods of expressing internal damping [7] which are not so widely used are:

1. Bluntness of the resonance curve.
2. A "frictional stress" related to the width of the hysteresis loop.
3. A frequency phase method [8].



## FACTORS AFFECTING INTERNAL DAMPING

The major difficulty noted by most investigators working in the field of material damping is the large number of parameters involved, and the apparent lack of relationships between them. The major parameters are listed below.

1. FREQUENCY. Although slight frequency effects have been noted, the great majority of investigators [7] have concluded that damping is entirely independent of frequency in the range of stresses of engineering significance.

2. STRESS AMPLITUDE. Amplitude of the stress is probably the most important single variable. Lazan [5] concluded that for many materials, the effect of stress magnitude (at constant temperature and stress history) may be expressed as

$$D = JS^N \quad (7)$$

where D is the specific damping energy in inch pounds per cubic inch per cycle, and S is the stress in pounds per square inch. J and N are constants which depend on the material. Lazan points out however that the value of J and N may vary widely for different materials.

3. STRESS DISTRIBUTION. Internal damping is not only a function of stress amplitude, but of stress distribution as well. For this reason many investigators have used thin walled tubes as test specimens, and subjected them to a torsional stress to achieve uniform stress throughout the specimen. Both Lazan [5] and Cochardt [6] have developed expressions for the resonance amplification factor in terms of a stress distribution function for some relatively simple shapes.

4. STRESS HISTORY. The effect of previous stress history has been noted by many investigators. The general indication is that the damping changes with repeated cycling, but approaches a constant value for any specific stress loading. Different materials are apparently affected in a different manner.

5. TEMPERATURE. Internal damping generally increases rapidly with increase in temperature over a wide range of temperatures [7]. An exception to this is magnetostrictive damping which is the subject of this report and is discussed in detail later.

6. NATURE OF THE STRESS. There is not much data available on variation in internal damping due to type of stress, but there is evidence that damping due to shearing stress is different than that under normal stress.

## MAGNETOSTRICTIVE DAMPING

Cochardt [9] noted that the origin of internal damping in metals has been traced to four sources.

1. Plastic flow
2. The thermoelastic effect
3. The magnetoelastic effect
4. Atomic Diffusion

In ferromagnetic alloys, only the magnetoelastic effect contributes significantly to the high internal damping in the stress and temperature range of engineering significance. The energy dissipated during a stress cycle as a result of the magnetoelastic effect is, according to Cochardt, generally caused by irreversible magnetostrictive strain.

Every ferromagnetic material contains so called domains or dipoles which are (in the absence of a magnetic field or a stress field) randomly oriented. When the material is subjected to a magnetic field, or a stress field, the domains tend to become aligned in the direction of the field. The re-orientation of these domains results in an irreversible change in the dimensions of the material which is termed magnetostriction.

The stress dependency of magnetostrictive strain is illustrated by figure 1, taken from Cochardt [9] which shows a stress strain hysteresis loop for a 50% CoFe alloy. Note that as the material is stressed in one direction and then cycled, the irreversible strain is of the order of 40 micro-inches per inch at approximately 10,000 pounds per square inch. If the stress level is increased above this limit, no further increase in irreversible strain occurs. The stress value at which this occurs is called the critical stress. The curve follows a hysteresis loop which is

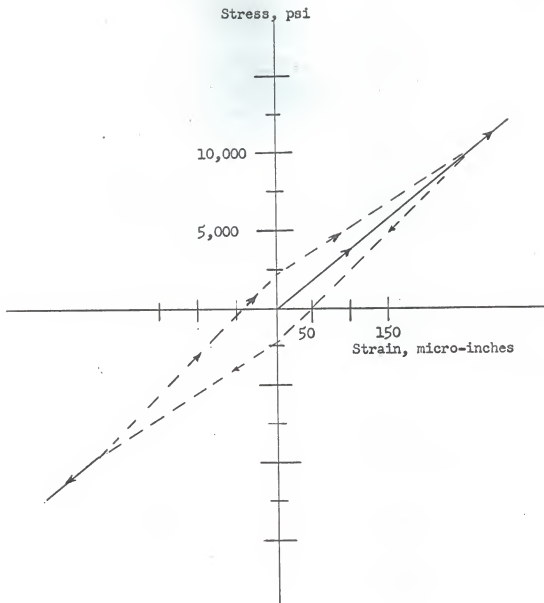


Figure 1. Stress Strain Diagram of a 50% CoFe strip under Static Load. From Cochardt, "The Origin of Damping in High Strength Ferromagnetic Alloys."

indicated by the dashed lines in Figure 1. The greater the area of the loop, the greater the internal damping of the material. From this it can be inferred [9] that the internal damping capacity of ferromagnetic alloys is a function only of magnetostriction and critical stress. The critical stress level is defined as the stress above which the area of the hysteresis loop remains constant.

Lazan [10] indicates that the energy dissipated as magnetostrictive damping may be much larger at low and intermediate stress than the damping caused by all other mechanisms. That this is true, has been shown by Cochardt and Lazan by magnetizing a specimen to saturation and observing that most of the damping disappears.

The presence of a static stress may also greatly reduce the damping in ferromagnetic materials. A static stress can suppress the motion of the domains and thus reduce damping as effectively as a magnetic field.

## EFFECT OF TEMPERATURE ON MAGNETOSTRICTIVE DAMPING

Most engineering materials show a decrease in magnetostrictive damping as the temperature is increased [10]. The rate of decrease is generally small at lower temperatures but as the curie temperature is approached the magnetostrictive damping falls off rapidly and approaches zero. There are exceptions to this behavior however, one being nickel which increases in damping with increasing temperature until about 390 degrees F, and then decreases rapidly and approaches zero as the curie temperature of 680 degrees F is reached.

## DEFINITION OF PROBLEM

The purpose of this report is to demonstrate magnetostrictive damping over a temperature range of 80 to 350 degrees F for two ferromagnetic alloys, mild steel and high carbon tool steel.

The two test specimens chosen were a 3/16 inch diameter mild steel welding rod and a 3/16 inch diameter drill rod. They were bent into a loop as shown in figure 2. to facilitate electrical heating. The rods were securely mounted to a heavy iron base and extended through the center of an electrical coil which was used to provide the magnetic field. The rods were given an initial displacement and released, and the rate of vibration decay was measured. Two resistance type strain gages were bonded to the rod and their output monitored on a Sanborn recorder. Rod temperature was measured from a thermocouple attached to the rod adjacent to the strain gages. Figures 3 and 4 show the test arrangement.

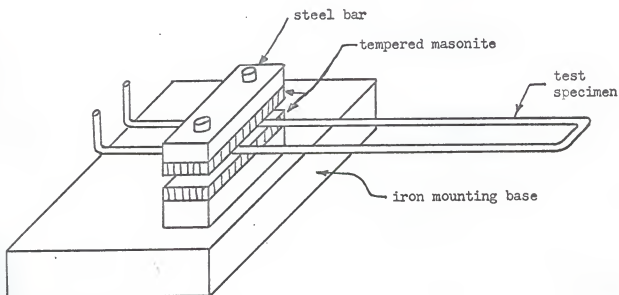


Figure 2. Test specimen mounting method.



Figure 3





Figure 4

## EXPERIMENTAL PROCEDURE

All tests were conducted at constant stress to insure that the variation in damping due to stress level (which is an important parameter) would not overshadow the effect of the magnetic field or the temperature. The stress level found to give the most consistent results for both specimens throughout the temperature range was 225 pounds per square inch.

The strain gage and recorder were first calibrated to measure stress directly as a function of recorder displacement, then preliminary tests were conducted to determine the saturation magnetization of the two specimens to insure that sufficient field strength existed to align the domains. Figures 13 and 14 show plots of the magnetization current. Since the rods were heated electrically, it was also necessary to determine if the interaction of the current flowing through the test specimen with the magnetic field would have any appreciable effect on the test. Immediately before each test at each temperature, the calibration was rechecked to insure good repeatability.

The mild steel specimen was tested first. At each temperature from room temperature to 350 degrees F in 50 degree increments, two test runs were made with the magnetic field and two test runs were made without the field. These tests were alternated so that no two tests with the field were conducted in sequence. The first time the mild steel specimen was tested, the data at the higher temperature were widely spread. (see figure 5). The test was repeated and the data from this second test was much better. It is felt that the improvement in the quality of the data is primarily due to improvement of the test technique and closer surveillance of the test temperature. See figure 6 for the results of the second mild steel test.

The test of the high carbon steel drill rod specimen was conducted using the same procedure established for the mild steel rod. A retest of the drill rod was also made in an effort to improve the quality of the data. The data for the drill rod sample are shown on figure 7. The combined data for both specimens are shown on figure 8.

Additional tests were conducted to determine if an appreciable time was required for the magnetic field to align the domains, and also to determine if the time required for the domains to become randomly oriented after the field was removed affected the test data. Lazan [10] found that the domains would "follow" a cyclic stress at frequencies up to hundreds of kilocycles, but no information was found which indicated the time required for the magnetic field to take effect.

In a few instances where a data point appeared to be too far removed from the norm, a re-check was made and in all cases the new data were found to fit closer to adjacent points.

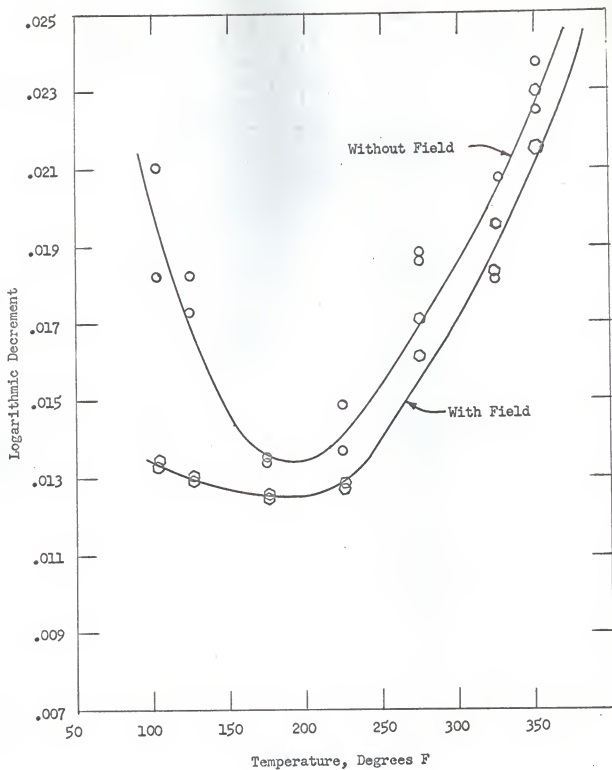


Figure 5. Logarithmic Decrement versus Temperature., 225 psi.

Test No. 1, Mild Steel Specimen.

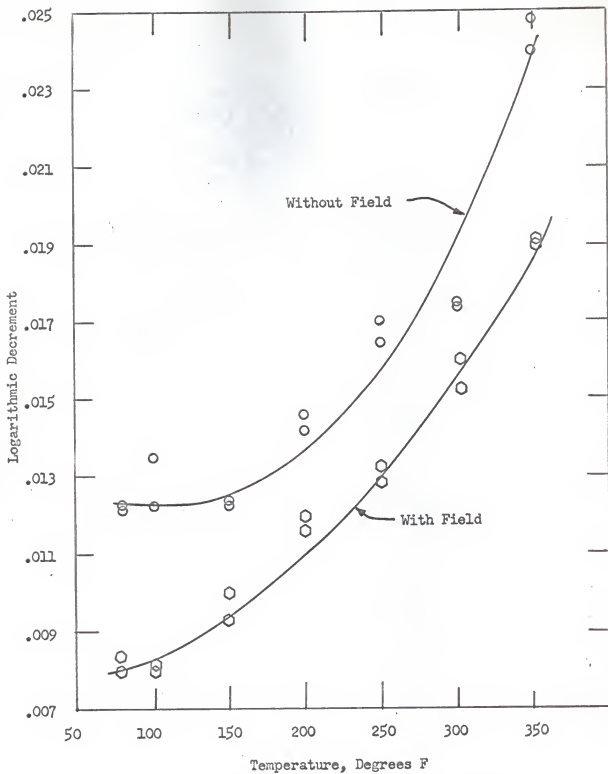


Figure 6. Logarithmic Decrement versus Temperature., 225 psi.

Test No. 2, Mild Steel Specimen.

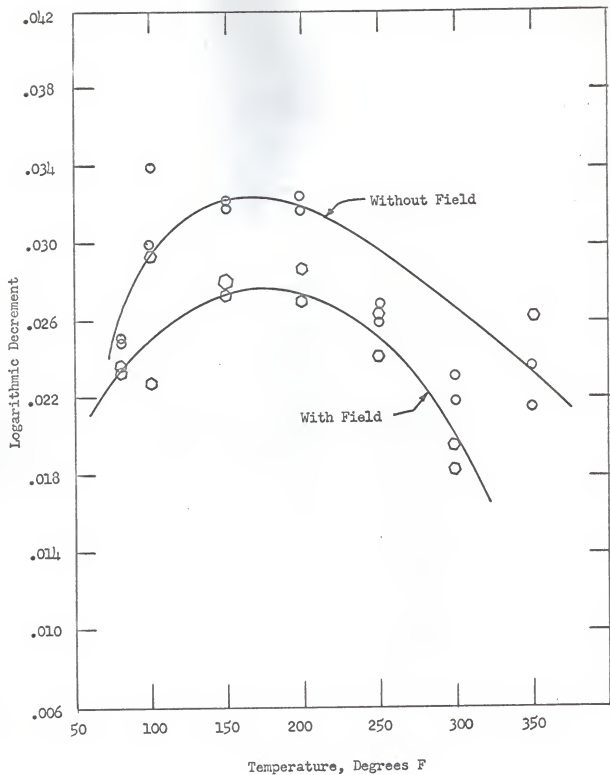


Figure 7. Logarithmic Decrement versus Temperature., 225 psi.  
Test No. 3, High Carbon Steel Specimen.

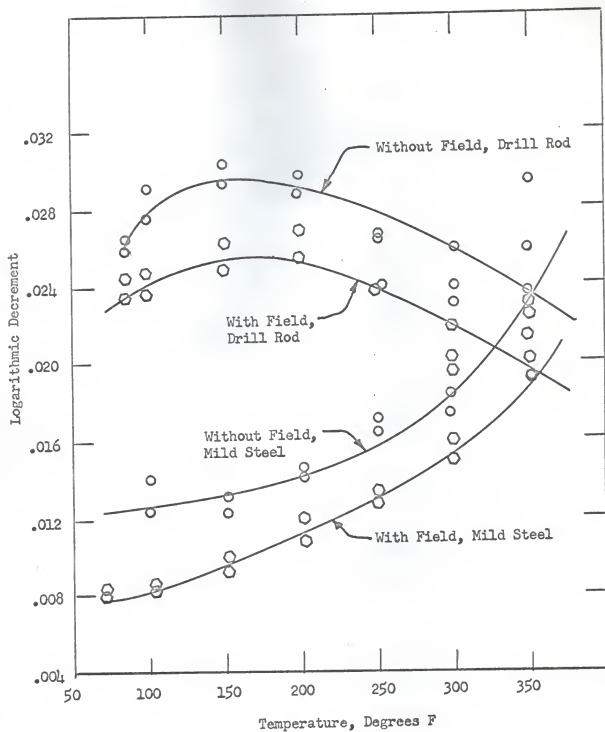


Figure 8. Combined Test Data, Logarithmic Decrement versus Temperature.,

225 psi.

## DISCUSSION OF RESULTS

The test results show conclusively that at a stress level of 225 pounds per square inch, the presence of the magnetic field significantly reduces the internal damping of both the test specimens. The damping characteristics of the two materials however are quite different. At room temperature the damping of the mild steel rod (as measured by the logarithmic decrement) was less than half the value for the high carbon tool steel rod. This result was expected however, since most of the literature describes the high strength alloys as being "high damping". Both Lazan [10] and Cochardt [9] have presented their data as a plot of damping versus stress at a single temperature. This experiment then, is purported to show what happens to one point of the damping-stress curve as the temperature is increased. Throughout the temperature range of this test, which is well below the curie temperatures of both materials, the damping of the mild steel rod increased with increasing temperature.

The theory [10] indicates that magnetostrictive damping decreases with increasing temperature up to the curie temperature where it reduces to zero. If the magnetostrictive damping does decrease with temperature, the two curves would draw closer together as the temperature is increased, or in other words, the effect of the magnetic field would decrease and if the temperature approached the curie temperature, the effect would disappear and the two curves would be coincident. For the temperature range used in this experiment, there was no obvious decrease in the magnetostrictive damping. It will probably be necessary to continue the experiment to higher temperatures to detect this effect.



The curves shown in Figure 8 do, however, show the general damping characteristics of the two materials at the 225 pound per square inch stress level. The general indication is that although the high carbon steel exhibits higher damping at room temperature, for temperatures above 350 degrees, the mild steel may have higher damping.

It must be remembered that the damping measured includes the external damping also which includes the energy absorbed by the support system and the viscous damping effect of the atmospheric air surrounding the vibrating beam. The part of the total damping effect which is attributed to magnetostrictive strain is the decrease in magnitude of the logarithmic decrement which results from applying the magnetic field.

## CONCLUSIONS

Although limitations of the experimental apparatus precluded testing the specimens at temperatures approaching the curie temperature, the results definitely show magnetostrictive damping to be a significant part of the total damping characteristic of both materials tested. However it should not be inferred from this experiment that at different stress levels or at higher temperatures that mild steel would have a higher damping capacity than high carbon steel, or that the general trends shown for the limited conditions of this test would hold true.

This experiment does do what was set out to do; that is, to demonstrate that magnetostrictive damping does occur and is significant at low to intermediate stress values and at temperatures below the curie temperature. It would be desirable to continue this test by extending the temperature range and testing a large number of high strength ferromagnetic materials.

#### ACKNOWLEDGEMENT

I express my appreciation to Dr. H. S. Walker of the Department of Mechanical Engineering, Kansas State University, for his guidance and counsel throughout the course of this work as my advisor.

I am grateful to my wife, Ruth, for her patience and understanding during the preparation of this report.

## REFERENCES

1. Sir William Thompson and Lord Kelvin, "On the Elasticity and Viscosity of Metals," Proceedings of the Royal Society of London, May 18, 1865.
2. Scientific Papers of Bertram Hopkinson, Cambridge University Press, London, England, 1921, pp. 99-107.
3. O. Pöppl, "The Practical Importance of the Damping of Metals, Especially Steels," Journal of the Iron and Steel Industries, Vol. 134, 1936, pp. 393-455.
4. B. J. Lazan, "Some Mechanical Properties of Plastics and Metals under Sustained Vibrations," ASME Transactions, Vol. 65, 1943, pp. 87-104.
5. B. J. Lazan, "Effect of Damping Constants and Stress Distribution on the Resonance Response of Members," ASME Transactions, Vol. 75, 1953, pp. 201.
6. A. W. Cochardt, "A Method for Determining the Internal Damping of Machine Members," ASME Transactions, Vol. 76, 1954, pp. 257.
7. J. M. Robertson and A. J. Yorgiadis, "Internal Friction in Engineering Materials," ASME Transactions, Vol. 68, 1946, pp. A-173.
8. H. D. Berns, "Frequency-Phase Method for Measuring Material Damping," A Master's Thesis, University of Nebraska, 1963.
9. A. W. Cochardt, "The Origin of Damping in High Strength Ferromagnetic Alloys," ASME Transactions, Vol. 75, 1953, pp. 196.
10. B. J. Lazan, "Damping and Resonance Fatigue Properties of Materials Considering Elevated Temperatures," Mechanical Behavior of Materials at Elevated Temperatures, McGraw Hill Book Co., Inc. New York, N.Y., 1961. pp. 477.

APPENDIX A

Calibration Procedure

## CALIBRATION PROCEDURE

The first step in the calibration was to calculate the maximum stress as a function of a concentrated load on the end of the cantilever beam. For the simple cantilever, the maximum stress is given by

$$S = \frac{M}{Z} = \frac{Pl}{Z} \quad (8)$$

For the doubled cross section, the sectional modulus is

$$Z = (2) \frac{\pi d^3}{32} \quad (9)$$

The rod diameter was 0.1875 inches and the beam length was 13.8 inches. Using these values, the stress-load relationship was found to be

$$S = 3750 P \quad (10)$$

where P is the load in pounds.

The beam was loaded progressively from 10 to 60 grams and the resulting deflection from the strain gage output on the Sanborn recorder was noted. This gave a direct relationship between maximum stress in the beam and deflection on the recorder which is independent of the gage factor and all other strain gage or recorder characteristics. The resonant frequency of the beam (approximately 23 cps), was well within the frequency response range of the recording instrument. For each series of tests a set of calibration curves was made. These calibration curves are included in this report as figures numbered 9, 10, 11, and 12. It is interesting to note that although the sensitivity decreased considerably at the higher temperatures, the response

remained linear. Figures 3 and 4 show the test setup with the calibration weights in place.

A copper-constantan thermocouple bonded to the rod adjacent to the strain gages was used to measure test temperature. The rod temperature was read out on a potentiometer with internal cold reference junction compensation, and the temperature was controlled by limiting the current flow through the rod with a variac which controlled the input to the current transformer.

The logarithmic decrement was calculated using the formula

$$\delta = \frac{1}{n} \ln \frac{A_0}{A_n} \quad (11)$$

In all cases during this experiment,  $n$  was taken to be 10. The procedure followed in determining the logarithmic decrement was as follows.

1. From the calibration curve, figures 9 through 12, determine the deflection corresponding to 225 psi at the test temperature.
2. Since this deflection is from zero to peak amplitude, and the amplitudes  $A_0$  and  $A_n$  are measured from peak to peak, multiply the deflection reading obtained by two.
3. Find the cycle on the Sanborn recording where the amplitude corresponds to 225 psi.
4. Measure the peak to peak amplitude after 10 cycles.
5. Using these values of  $A_0$  and  $A_n$  and setting  $n$  equal to 10 calculate the logarithmic decrement from formula (1).

Figure 9. Calibration Curves.  
Maximum Stress versus Deflection.  
Test No. 1, Mild Steel

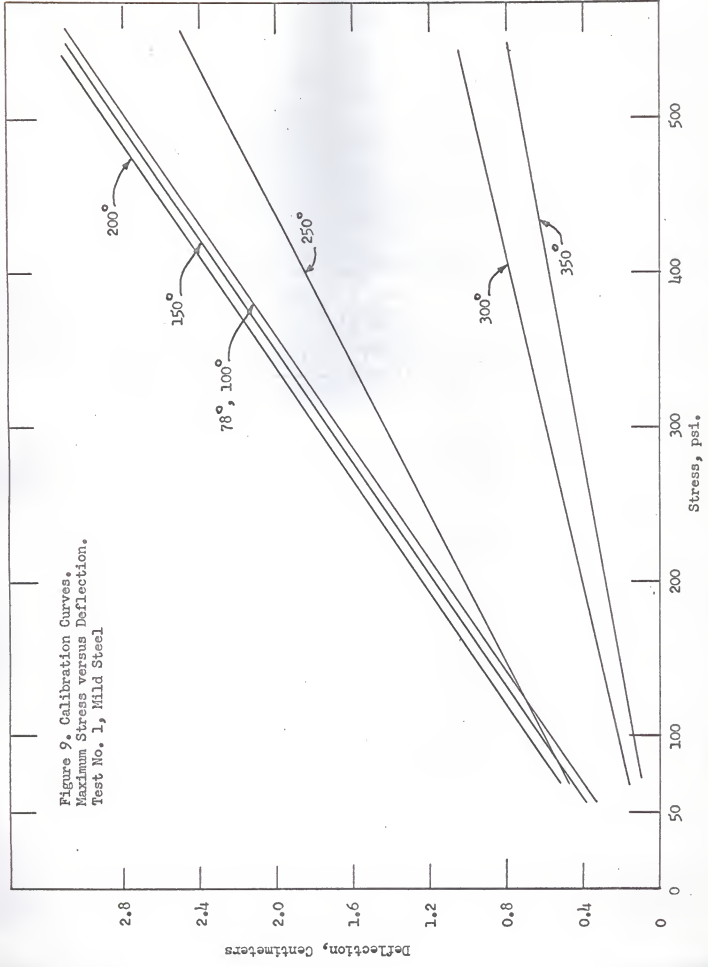




Figure 10. Calibration Curves.  
Maximum Stress versus Deflection  
Test No. 2, Mild Steel

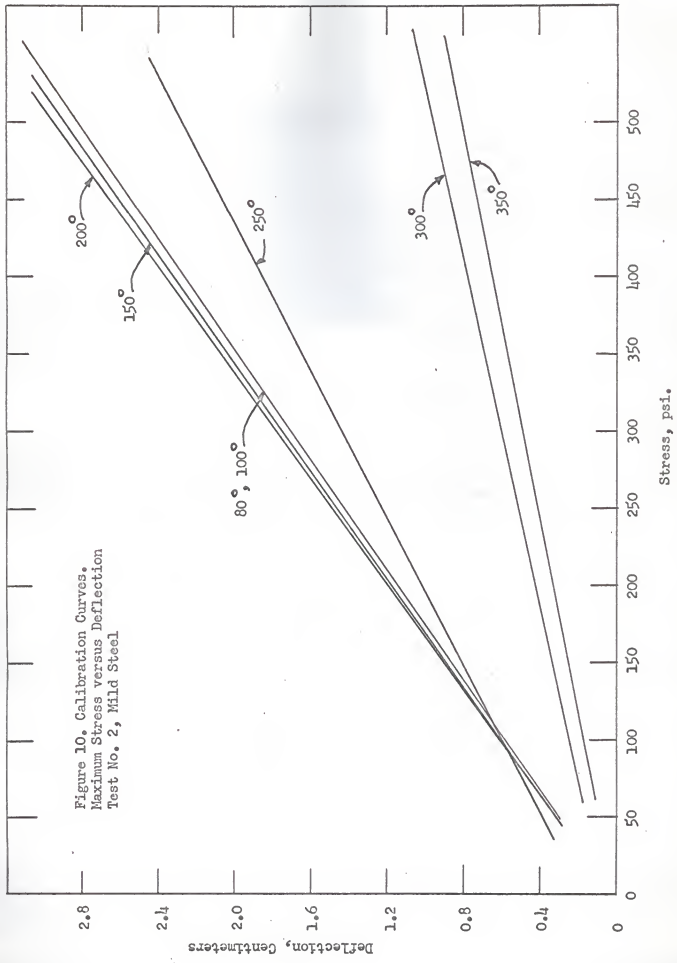


Figure 11. Calibration Curves.  
Maximum Stress Versus Deflection  
Test No. 3, High Carbon Steel

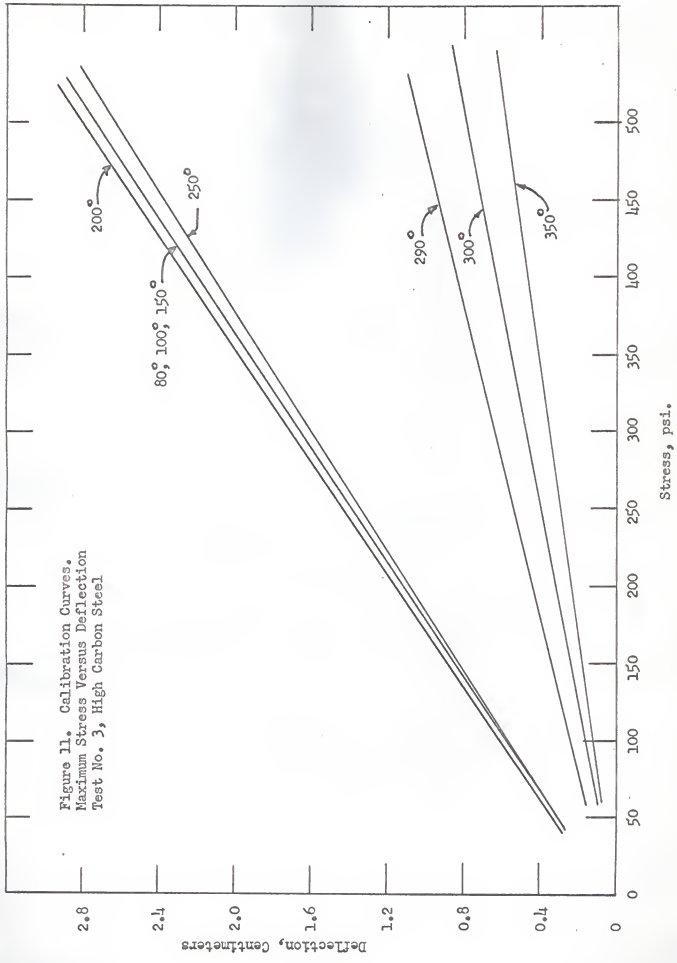
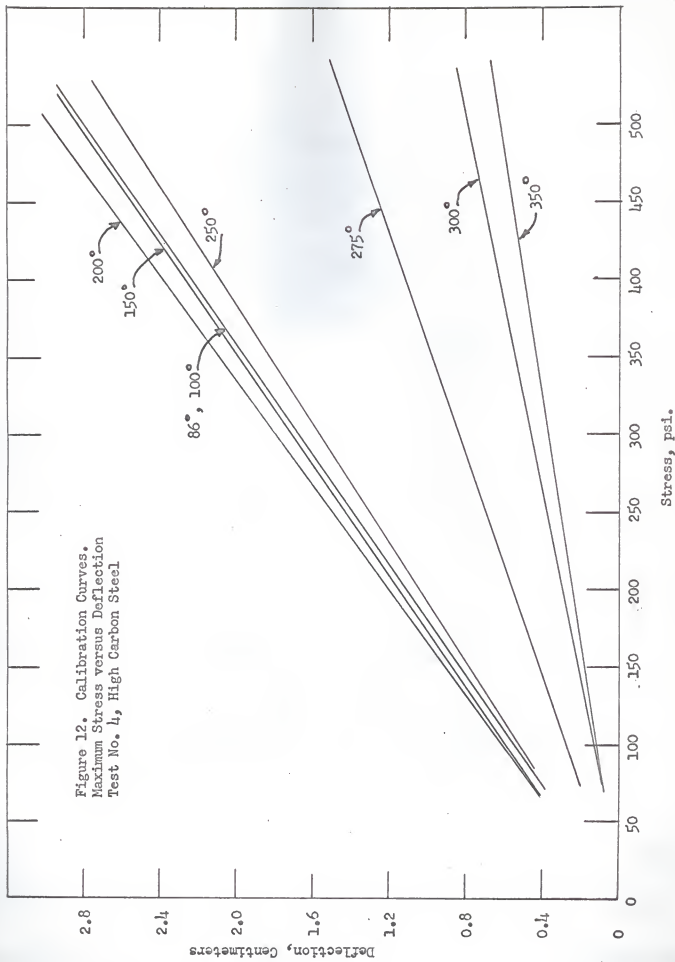


Figure 12. Calibration Curves.  
Maximum Stress versus Deflection  
Test No. 4, High Carbon Steel



APPENDIX B

Equipment List

## EQUIPMENT LIST

The following is a list of the equipment and measuring instruments used during this experiment. Numbers refer to the notation on figure 3.

1. Sanborn Recorder model no. 60-1300B, with Sanborn Strain Gage Amplifier, model no. 64-500B.
2. Variac, 240 volt input, 0-240 volt output, 10 amp maximum.
3. AC Ammeter, variable range, 1 amp to 50 amp full scale.
4. Current Transformer, Weston model no. 15964.
5. Millivolt Potentiometer, Leeds and Northrop, Catalog no. 8686.
6. Cast iron mounting base.
7. Precision metric balance weights.
8. Heavy duty electrical coil.
9. DC Ammeter, Weston variable range, 10 amp to 100 amp full scale.
10. DC Power Supply, Consolidated Electrodynamics Corporation, variable range.

The strain gages used were Baldwin SR-4, type FA-12-12, 1/4 inch gage length. The gages were bonded to the test specimens with high temperature epoxy cement.

APPENDIX C

Typical Data

TYPICAL DATA

Calibration Data: Stress = 3750(P), where P is the load in pounds.

<u>Load, lbs.</u>	<u>Deflection, cm.</u>	<u>Stress, psi.</u>
0.022046	0.19	82.67
0.04409	0.93	165.34
0.06613	1.39	248.01
0.08818	1.82	330.68
0.11023	2.27	413.35

High Carbon Steel Drill Rod, Test No. 3. Experimental data.

<u>Temp.</u>	<u>Stress</u>	<u>A</u>	<u>A</u>	<u>δ</u>	<u>Field*</u>
80	225	2.5	1.92	0.0264	WO
80	225	2.5	1.90	0.0274	W
80	225	2.5	1.90	0.0274	WO
80	225	2.5	1.90	0.0274	W
150	225	2.5	1.82	0.0318	WO
150	225	2.5	1.89	0.028	W
150	225	2.5	1.81	0.0323	WO
150	225	2.5	1.90	0.0274	W
200	225	2.58	1.88	0.0324	WO
200	225	2.58	1.97	0.02695	W
200	225	2.58	1.88	0.0324	WO
200	225	2.58	1.94	0.0285	W
250	225	2.42	1.85	0.0268	WO
250	225	2.42	1.90	0.0241	W
250	225	2.42	1.86	0.0263	WO
250	225	2.42	1.87	0.0258	W
300	225	1.02	0.81	0.023	WO
300	225	1.02	0.84	0.0195	W
300	225	1.02	0.82	0.0218	WO
300	225	1.02	0.85	0.01825	W
350	225	0.52	0.41	0.0237	WO
350	225	0.52	0.40	0.0262	W
350	225	0.52	0.42	0.0214	WO
350	225	0.52	0.41	0.0237	W

\* W means with magnetic field, WO means without the field.

APPENDIX D

Determination of Magnetic Saturation



## DETERMINATION OF MAGNETIC SATURATION

Before the calibration could be performed or the test conducted, it was necessary to perform saturation tests on both the mild steel and the high carbon steel specimens to insure that adequate current was available to provide a sufficiently strong magnetic field to completely align the domains in the material. For both specimens, a definite saturation level was found. Saturation current for the mild steel was found to be approximately 1.2 amperes, and for the high carbon steel, about 0.1 amperes. The saturation level apparently does not vary with temperature.

All the tests were conducted with 5.5 amperes flowing through the coil so that it is highly probable that the domains were completely aligned for all tests with the field on. Figures 13 and 14 show the magnetization curves.

Figure 13. Saturation Current versus Logarithmic Decrement, Mild Steel Specimen.

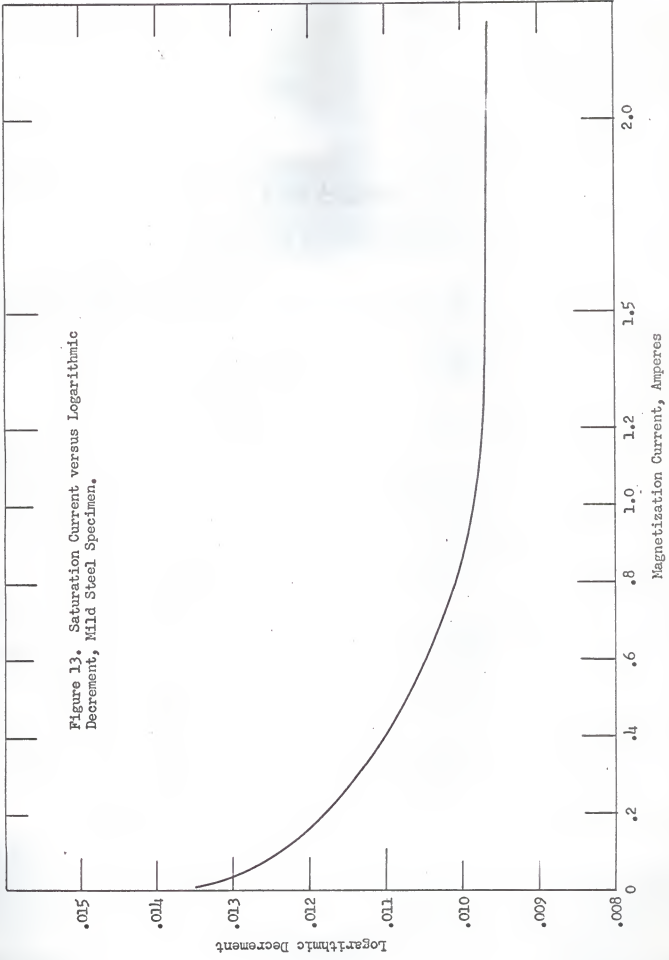
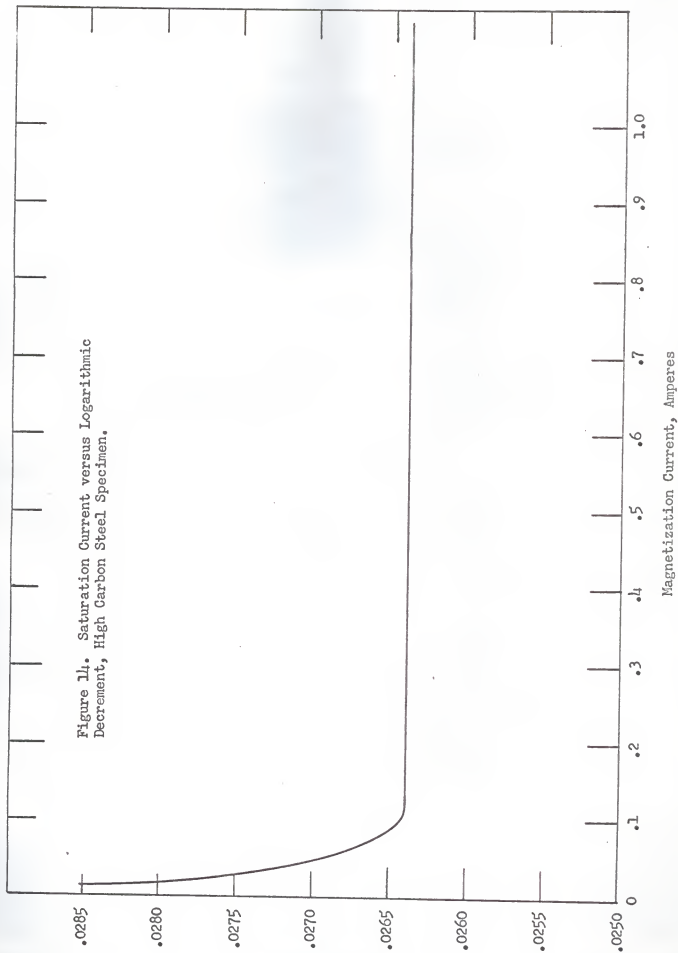


Figure 14. Saturation Current versus Logarithmic Decrement, High Carbon Steel Specimen.



APPENDIX E

Derivation of the  
Logarithmic Decrement

DERIVATION OF THE LOGARITHMIC DECREMENT

The general equation for a free damped vibration of a simple spring mass system is given as

$$m\ddot{x} + c\dot{x} + kx = 0 \quad (12)$$

To obtain a solution to this equation, assume a solution of the form.

$$x = Ae^{\alpha t} \quad (13)$$

Differentiate this expression twice and substitute back into equation (11).

$$\dot{x} = \alpha Ae^{\alpha t}$$

$$\ddot{x} = \alpha^2 Ae^{\alpha t}$$

$$m\alpha^2 Ae^{\alpha t} + c\alpha Ae^{\alpha t} + kAe^{\alpha t} = 0$$

Divide each term of this expression by

$$m Ae^{\alpha t}$$

and the following quadratic equation results.

$$\alpha^2 + \frac{c}{m}\alpha + \frac{k}{m} = 0 \quad (14)$$

This equation has the roots

$$\alpha_{1,2} = -\frac{c}{2m} \pm \frac{1}{2} \sqrt{\left(\frac{c}{m}\right)^2 - \frac{4k}{m}}$$

which simplifies to

$$\alpha_{1,2} = -\frac{c}{2m} \pm \frac{1}{2m} \sqrt{c^2 - 4km}$$

the solution (12) is then seen to be

$$x = Ae^{(-\frac{c}{2m} + \frac{1}{2m}\sqrt{c^2 - 4km})t} + Be^{(-\frac{c}{2m} - \frac{1}{2m}\sqrt{c^2 - 4km})t} \quad (15)$$

The algebraic sign of the quantity  $\sqrt{c^2 - 4km}$  determines the type of motion that will occur. For an oscillatory motion,  $4km > c^2$  and  $\sqrt{c^2 - 4km}$  will be imaginary. In this case  $\alpha_1$  and  $\alpha_2$  become

$$\alpha_1 = -\frac{c}{2m} + \frac{i}{2m}\sqrt{4km - c^2} \quad (16)$$

$$\alpha_2 = -\frac{c}{2m} - \frac{i}{2m}\sqrt{4km - c^2} \quad (17)$$

Now define  $\sqrt{4km - c^2}$  to be the damped natural frequency  $\omega$ , then the following simplifications follow

$$x = Ae^{-\frac{c}{2m}t} e^{i\frac{\omega}{2m}t} + Be^{-\frac{c}{2m}t} e^{-\frac{i\omega}{2m}t}$$

$$x = e^{-\frac{c}{2m}t} \left[ A(\cos \frac{\omega}{2m}t + i \sin \frac{\omega}{2m}t) + B(\cos \frac{\omega}{2m}t - i \sin \frac{\omega}{2m}t) \right]$$

$$x = e^{-\frac{c}{2m}t} \left[ \cos \frac{\omega}{2m}t (A+B) + i \sin \frac{\omega}{2m}t (A-B) \right]$$

$$C_1 = (A+B)$$

$$C_2 = (A-B)$$

$$x = e^{-\frac{c}{2m}t} \left[ C_1 \cos \frac{\omega}{2m}t + C_2 i \sin \frac{\omega}{2m}t \right] \quad (18)$$

Now consider the amplitude at time  $t$  and at time  $t + T$ , where  $T$  is the period of vibration and is defined to be

$$T = \frac{2\pi}{\omega} \quad (19)$$

Now form the ratio

$$\frac{x(t)}{x(t+T)} = \frac{e^{-\frac{c}{2m}t}}{e^{-\frac{c}{2m}(t+\frac{2\pi}{\omega})}}$$

The sin and cos terms cancel since

$$\cos \frac{\omega}{2m}t = \cos \frac{\omega}{2m}(t+T)$$

$$\sin \frac{\omega}{2m}t = \sin \frac{\omega}{2m}(t+T)$$

the ratio then reduces to

$$\frac{x(t)}{x(t+T)} = e^{\left[-\frac{c}{2m}t + \frac{c}{2m}t + \frac{c}{2m}\left(\frac{2\pi}{\omega}\right)\right]}$$

$$\frac{x(t)}{x(t+T)} = e^{\frac{c\pi}{m\omega}} \quad (20)$$

The logarithmic decrement,  $\delta$ , is defined as

$$\delta = \frac{1}{n} \ln \frac{x(t)}{x(t+nT)} = \ln e^{\frac{c\pi}{m\omega}}$$

For this case  $n = 1$  and the logarithmic decrement is

$$\delta = \frac{c \pi}{m \omega} \quad (21)$$

or the damping coefficient,  $c$ , is expressible as

$$c = \frac{\delta m \omega}{\pi} \quad (22)$$



MAGNETOSTRICTIVE DAMPING OF TWO FERROMAGNETIC  
ALLOYS AT ELEVATED TEMPERATURES

by

NEWTON REED ANDERSON

B.S., Kansas State University, 1958

---

AN ABSTRACT OF A MASTER'S REPORT

submitted in partial fulfillment of the  
requirements for the degree

MASTER OF SCIENCE

Department of Mechanical Engineering

KANSAS STATE UNIVERSITY  
Manhattan, Kansas

1966

The vibration decay rate of two ferromagnetic alloys is measured in a strong magnetic field to demonstrate magnetostrictive damping. The magnetic field aligns the magnetic domains in the material and substantially reduces the internal damping. Vibration decay measurements were made at temperatures from 80 to 350 degrees F at a stress level of 225 pounds per square inch.